Development 138, 5257-5267 (2011) doi:10.1242/dev.069062

A conserved PTEN/FOXO pathway regulates neuronal morphology during *C. elegans* development

Ryan Christensen[1], Luis de la Torre-Ubieta[2], Azad Bonni[2] and Daniel A. Colón-Ramos[1,*]

SUMMARY

The phosphatidylinositol 3-kinase (PI3K) signaling pathway is a conserved signal transduction cascade that is fundamental for the correct development of the nervous system. The major negative regulator of PI3K signaling is the lipid phosphatase DAF-18/PTEN, which can modulate PI3K pathway activity during neurodevelopment. Here, we identify a novel role for DAF-18 in promoting neurite outgrowth during development in *Caenorhabditis elegans*. We find that DAF-18 modulates the PI3K signaling pathway to activate DAF-16/FOXO and promote developmental neurite outgrowth. This activity of DAF-16 in promoting outgrowth is isoform-specific, being effected by the *daf-16b* isoform but not the *daf-16a* or *daf-16d/f* isoform. We also demonstrate that the capacity of DAF-16/FOXO in regulating neuron morphology is conserved in mammalian neurons. These data provide a novel mechanism by which the conserved PI3K signaling pathway regulates neuronal cell morphology during development through FOXO.

KEY WORDS: FOXO, PTEN, Axon outgrowth, Dendrite morphology, Neurodevelopment

INTRODUCTION

The phosphatidylinositol 3-kinase (PI3K) signaling pathway is a conserved signal transduction cascade that is essential for proper nervous system development (Cosker and Eickholt, 2007; Eickholt et al., 2007; Shi et al., 2003; van der Heide et al., 2006; Waite and Eickholt, 2010). Activation of the PI3K signaling pathway relies on activation of class I PI3-kinase, which generates signaling intermediate molecule PIP_3 (phosphatidylinositol 3,4,5-trisphosphate) (Vanhaesebroeck et al., 2001). PIP_3 mediates the recruitment and activation of kinases, adaptor proteins and small GTPases to regulate neurodevelopmental responses ranging from cell survival to synaptic development.

The dual specificity phosphatase PTEN dephosphorylates PIP_3 to antagonize the PI3K signaling pathway (Li et al., 1997; Maehama and Dixon, 1998). PTEN is highly expressed in the nervous systems of animals, and regulation of PI3K signaling by PTEN is crucial for neurodevelopment (Gimm et al., 2000; Lachyankar et al., 2000; Masse et al., 2005). In *Caenorhabditis elegans*, the PI3K/PTEN pathway regulates neuronal polarization prior to axon outgrowth (Adler et al., 2006). The PI3K/PTEN pathway regulates cell size, branching and polarization in cultured neuronal cells (Higuchi et al., 2003; Jia et al., 2010; Lachyankar et al., 2000; Musatov et al., 2004). *Pten* deletion in mouse neurons results in neuronal hypertrophy, ectopic axon formation and excessive branching (Backman et al., 2001; Fraser et al., 2004; Kwon et al., 2006; Kwon et al., 2001; van Diepen and Eickholt, 2008). Inactivating mutations of *PTEN* in humans result in neurological defects such as mental retardation, ataxia and seizures (Arch et al., 1997; Liaw et al., 1997; Marsh et al., 1997). Therefore, PTEN plays a conserved role in regulating the development and wiring of the nervous system.

The PI3K/PTEN pathway relies primarily on the modulation of cytoskeletal dynamics and mTOR-dependent protein synthesis to instruct neuronal morphogenesis (Cosker and Eickholt, 2007; van Diepen and Eickholt, 2008). The increase in neuronal cell size observed in *Pten*-null neurons can be reversed by treatment with an mTOR inhibitor (Kwon et al., 2003; Zhou et al., 2009), suggesting that the effects of *Pten* deletion on neurodevelopment are mediated primarily through PI3K-derived mTOR activation and protein synthesis. Interestingly, in neuron-specific *Pten* knockout mice, granule cells of the dentate gyrus show a loss of neuronal polarity even after rapamycin treatment, suggesting mTOR-independent pathways could also be involved in PTEN-mediated neurodevelopment (Zhou et al., 2009). The identity of these mTOR-independent pathways is currently unknown.

Here, we identify a novel pathway by which PTEN regulates neuronal morphology and outgrowth during development. We first report a novel role for DAF-18/PTEN in promoting neurite outgrowth during development in *C. elegans*. This novel function adds to PTEN's known role in inhibiting axon outgrowth through mTOR-dependent pathways (Kwon et al., 2003; Zhou et al., 2009). We find that DAF-18 promotes axon outgrowth in *C. elegans* through an mTOR-independent pathway. Our data indicate that DAF-18 modulates the PI3K signaling pathway to activate DAF-16/FOXO and promote developmental axon outgrowth. Importantly, we show that this novel role of DAF-16 in developmental outgrowth is mediated by a specific isoform, DAF-16B. We also demonstrate that this outgrowth-promoting role of DAF-16/FOXO is conserved in mammalian neurons.

MATERIALS AND METHODS

Strains and genetics

Worms were raised at room temperature using OP50 *Escherichia coli* seeded on NGM plates. Strains with a *pdk-1(sa680)* or *daf-2(e1370)* mutation were raised at a permissive temperature of 16°C and analyzed at

[1]Program in Cellular Neuroscience, Neurodegeneration and Repair, Department of Cell Biology, Yale University School of Medicine, P.O. Box 9812, New Haven, CT 06536-0812, USA. [2]Department of Neurobiology, Harvard Medical School, New Research Building, Room 856, 77 Ave. Louis Pasteur, Boston, MA 02115, USA.

*Author for correspondence (daniel.colon-ramos@yale.edu)

Accepted 7 October 2011

22°C or 25°C, respectively. To control for maternal rescue in the first generation, *age-1(mg44)* and *daf-18(mg198); age-1(mg44)* mutants were analyzed as second-generation *age-1(mg44)* homozygotes. N2 Bristol was utilized as the wild-type reference strain. Strains obtained through the *Caenorhabditis* Genetics Center include: GR1032 *age-1(mg44) II/mnC1 dpy-10(e128) unc-52(e444) II*, VC204 *akt-2(ok393) X*, GR1308 *daf-16(mg54) I; daf-2(e1370) III*, JT9609 *pdk-1(sa680) X*, KR344 *let-363(h98) dpy-5(e61) unc-13(e450) I; sDp2(I;f)*, HT1881 *daf-16(mgDF50) I; daf-2(e1370) unc-119(ed3) III; lpIS12*, HT1882 *daf-16(mgDF50) I; daf-2(e1370) unc-119(ed3) III; lpIS13*, HT1883 *daf-16(mgDF50) I; daf-2(e1370) unc-119(ed3) III; lpIS14*, KQ1366 *rict-1(ft7) II*, CF1038 *daf-16(mu86) I*, VC1027 *daf-15(ok1412)/nT1 IV; +/nT1 V*, CB1370 *daf-2(e1370) III*. SO26 *daf-18(mg198) IV* was provided by the Solari laboratory, Centre Leon Berard, Leon, France. GR1309 *daf-16(mgDF47) I; daf-2(e1370) III* was provided by the Ruvkun laboratory, Boston, MA, USA. OH99 *mgIS18 IV* and LE311 *lqIS4 X* were provided by the Hobert laboratory, New York, NY, USA. FX00399 *akt-1(tm399) V* was provided by the Japanese Knockout Consortium, Tokyo, Japan.

Molecular biology and transgenic lines

Expression clones were made in the pSM vector, a derivative of pPD49.26 (A. Fire, Stanford University School of Medicine, Stanford, CA, USA) with extra cloning sites (S. McCarroll and C. I. Bargmann, unpublished data). The plasmids and transgenic strains (0.5-30 ng/μl) were generated using standard techniques and co-injected with markers *Punc-122::gfp* or *Punc122::dsRed* (15- 30 ng/μl): *wyIs45 [Pttx3::gfp::rab3]*, *wyIs92 [Pmig-13::snb-1::yfp+odr-1::rfp]*, *olaEx20 [Pttx3::mch, Pglr3::mch, Pdaf-18::daf-18 cDNA, Punc-122::GFP]*, *olaEx25 [Pttx3::mch, Pglr3::mch, Pdaf-18::daf-18 cDNA, Punc-122::GFP]*, *olaEx72 [Pttx-3b::daf-18 cDNA, punc-122::GFP]*, *olaEx73 [Pttx-3b::daf-18 cDNA, Punc-122::GFP]*, *olaEx528 [Pttx-3b::GFP, Punc-122::GFP]*, *olaEx529 [Pttx-3b::GFP, Punc-122::GFP]*, *olaEx531 [Pttx-3b::GFP, Punc-122::GFP]*, *olaEx532 [Pttx-3b::GFP, Punc-122::GFP]*, *olaEx533 [Pttx-3b::GFP, Punc-122::GFP]*, *olaEx534 [Pttx-3g::HRP::CD2::GFP, Punc-122::GFP]*, *olaEx760 [Pttx-3g::GFP, Punc-122::GFP]*, *olaEx761 [Pttx-3g::GFP, Punc-122::GFP]*, *olaEx762 [Pttx-3g::GFP, Punc-122::GFP]*, *olaEx763 [Pttx-3g::mCH, Pdaf-16b::GFP]*, *olaEx764 [Pttx3::mch, Pglr3::mch, cosmid R13H8, Punc-122::GFP]*.

Fluorescence microscopy and confocal imaging

Images of fluorescently tagged fusion proteins were captured in live *C. elegans* using a 60× CFI Plan Apo VC, NA 1.4, oil objective on an UltraView VoX spinning disc confocal microscope (PerkinElmer). Worms were immobilized using 50 nM levamisole (Sigma), oriented anterior to the left and dorsal up.

Mosaic analysis

Mosaic analysis was conducted on *daf-18(mg198)* or *daf-16(mgDF47)* animals as described previously by expressing unstable transgenes with the rescuing *pdaf-18::daf-18* cDNA (Solari et al., 2005) or cosmid R13H8 (for *daf-16* mosaics), and cytoplasmic cell-specific markers in RIA and AIY (Colon-Ramos et al., 2007; Yochem and Herman, 2003). Animals were inspected for retention of the transgene and rescue using a Leica DM5000 B microscope.

Quantification

Quantification of AIY outgrowth in wild-type and mutant animals was carried out on a Leica DM5000 B microscope. Neurite truncations were scored as a failure of the two AIY neurites to meet at the dorsal midline. Neurite outgrowth in embryos was quantified by measuring the length of the whole neurite and Zone 3 (dorsal portion of the neurite) regions in confocal micrographs using Volocity 5 software (Improvision). Zone 3 length was averaged using images of several embryos (three to six) taken at each developmental time point, with individual Zone 3 lengths determined as described above. Embryos were assigned a stage based on morphological characteristics and developmental time points, such as the beginning of twitching.

Quantification of AIY neurite length in wild-type, *daf-18(mg198)*, *daf-16(mgDF47)*; and *daf-16(mgDF47); daf-18(mg198)* L4 animals was carried out by imaging the length of the dorsal portion of both AIY axons (Zone 2 and Zone 3) using a 60× CFI Plan Apo VC, NA 1.4, oil objective on an UltraView VoX spinning disc confocal microscope (PerkinElmer). Zone 2 and Zone 3 were defined as the portion of the AIY neurite that turned and extended dorsally, respectively. These regions were measured in 3D by using Volocity software (Improvision).

Statistical significance was calculated using Student's *t*-test or Fisher's Exact Test.

Transfection and immunocytochemistry

Primary cerebellar granule neurons were prepared from P6 Long Evans rat pups as described (Konishi et al., 2002). One day after culture preparation, neurons were treated with cytosine arabinofuranoside (AraC) at a final concentration of 10 μM to prevent glial proliferation. Granule neurons were transfected using a modified calcium phosphate method as described (de la Torre-Ubieta et al., 2010). Cells were fixed at the indicated time points and subjected to immunocytochemistry with the GFP (Molecular Probes) antibody together with the MAP2 (Sigma) or Tau1 (Chemicon) antibodies, and stained with the DNA-binding dye bisbenzimide (Hoechst 33258).

Morphological analysis of cerebellar granule neurons

To characterize the morphology of cerebellar granule neurons, individual images were captured randomly and in a blinded manner on a Nikon eclipse TE2000 epifluorescence microscope using a digital CCD camera (Diagnostic Instruments). Images were imported into Spot Imaging Software (Diagnostic Instruments) and the length of neuronal processes was analyzed by tracing. Total length is the length of processes including all its branches added together for a given neuron. To analyze neuron polarization, neurons were scored in a blinded manner as polarized or non-polarized as previously described (de la Torre-Ubieta et al., 2010; Shi et al., 2003). A neuron in which the longest neurite was at least twice as long as the other neurites was considered to be polarized. Data were collected from three independent experiments with 50-100 neurons scored per condition per experiment.

RNAi and rescue constructs

A DNA template-based method of RNAi was used to express short hairpin RNAs (shRNAs) targeting the sequence GAGCGTGCCCTACTTCAAGG in FOXO1, FOXO3 and FOXO6 (de la Torre-Ubieta et al., 2010). Sequences for the scrambled shRNAs are TACGC-GCATAAGATTAGGGTG (U6/scr1) and AAGTGCCAATTTCG-ATGATAT (U6/scr2). The rescue construct for FOXO6 (FOXO6-Res) was generated by engineering silent mutations (indicated by bold font) on FOXO6 as follows: CGT**C**CCC**G**TA**T**TTCAAGG (de la Torre-Ubieta et al., 2010).

Statistics

Statistical analyses were performed using GraphPad software. In experiments in which only two groups were analyzed, comparison of the two groups was carried out using Student's *t*-test. Pairwise comparison within multiple groups was carried out by analysis of variance (ANOVA) followed by the Bonferroni post-hoc test. All histogram data were obtained from three or more independent experiments and are presented as mean ± s.e.m. unless otherwise specified. Statistical information and the total number of cells analyzed per experiment are provided in the figure legends.

RESULTS

DAF-18 is required for neurite length

The AIY interneurons are a pair of interneurons that modulate temperature response in the nematode (Mori and Ohshima, 1995; White et al., 1986) (Fig. 1A). These neurons are embedded in the nerve ring and show great specificity at the level of morphological development and synaptic partner connectivity (Altun-Gultekin et al., 2001; White et al., 1986). In wild-type animals, the morphology of AIY is exquisitely stereotyped across individual animals (n>500 animals). This facilitates genetic analysis and allows examination of molecules required for neurodevelopment in vivo with single-cell resolution (Altun-Gultekin et al., 2001; Colon-Ramos et al., 2007).

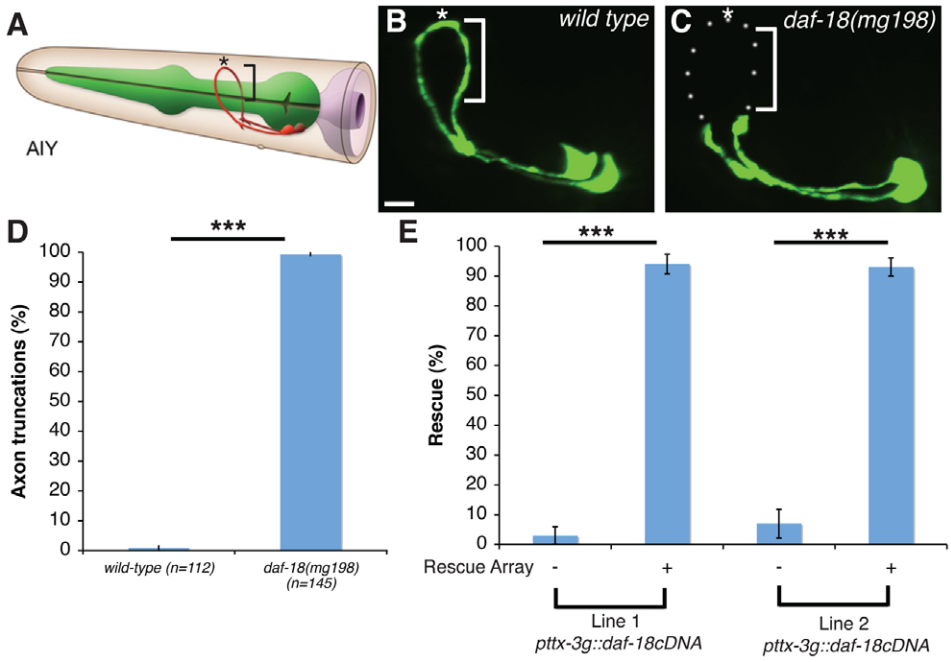

Fig. 1. DAF-18/PTEN acts cell-autonomously to control neurite length in the AIY interneurons. (**A**) Schematic of wild-type AIY morphology and location in the nematode nerve ring. Asterisk marks location where two AIY interneurons (red) meet at the dorsal midline (White et al., 1986). Bracket denotes portion of AIY neurite truncated in *daf-18(mg198)* mutants. Adapted with permission from Zeynep Altun (www.wormatlas.org). Green, pharynx; red, AIY interneurons. (**B**,**C**) Confocal micrographs of AIY morphology in wild-type (B) and *daf-18(mg198)* mutant (C) animals, visualized with cytoplasmic GFP expressed cell-specifically in AIY (*pttx-3b::GFP*). The three-dimensional reconstructions of the micrographs are oriented as the schematic representation in A to show both bilaterally symmetric AIYs. Note the missing dorsal portion of neurites in *daf-18(mg198)* animal compared with wild type (brackets). Asterisk denotes location of dorsal midline. (**D**) Percentage of animals with truncated neurites in wild type (n=112) and *daf-18(mg198)* mutants (n=145). (**E**) Cell-specific rescue of the *daf-18* phenotype in AIY. Transgenic *daf-18(mg198)* mutant animals expressing a *daf-18* cDNA rescue construct (*pttx-3g::daf-18 cDNA*) cell-specifically in AIY were created and the percentage of animals with neurite truncations were quantified. Shown here are the results from two independently generated transgenic lines. As a control we also show the quantification of siblings not carrying the rescuing array. Note how cell-specific expression of *daf-18* cDNA in AIY effectively rescued the neurite length defect seen in *daf-18(mg198)* mutants. ***P<0.001 between indicated groups. Error bars represent s.e.m. Scale bar: 5 μm.

To gain insight into molecular mechanisms that control neurodevelopment, we screened mutants for their requirement in AIY development. We focused on the PI3K signaling pathway for three reasons: (1) components of the PI3K pathway have been shown to regulate numerous neurodevelopmental processes, including neuronal cell size, neurite outgrowth and synapse formation (Cosker and Eickholt, 2007; Waite and Eickholt, 2010); (2) components of the PI3K pathway are well conserved throughout evolution (MacDougall et al., 1995; Morris et al., 1996; Vanhaesebroeck et al., 1997); and (3) components of the PI3K pathway act cell-autonomously in AIY to regulate behaviors (Kodama et al., 2006; Murakami et al., 2005).

To determine the role of the PI3K signaling pathway in AIY neurodevelopment, we first examined mutants in genes that promote PI3K signaling. Loss of function mutations in *age-1(mg44)*, *akt-1(tm399)* and *akt-2(ok393)* were examined for defects in AIY morphology and synapse formation. Even after careful inspection of cell migration, axon guidance and synapse localization, we could not detect any major defects in the neurodevelopmental decisions made by AIY with these alleles (supplementary material Fig. S1; n>40 animals for each examined allele).

We then examined whether DAF-18, the primary negative regulator of PI3K signaling, was required for AIY neurodevelopment. We examined the putative null allele *daf-18(mg198)* and observed a highly penetrant AIY neurite length defect. In wild-type animals, the bilaterally symmetric AIYs extend neurites that meet at the dorsal midline. This phenotype is very stereotypical across wild-type animals (111 out of the 112 animals examined displayed the reported phenotype) (Fig. 1B,D). By contrast, in almost all of the *daf-18(mg198)* mutant animals AIY failed to reach the dorsal midline (144 out of 145 animals examined had AIY neurites that did not reach the dorsal midline) (Fig. 1C,D). We quantified neurite length and observed that the average length of AIY neurites in *daf-18(mg198)* animals is half of that in wild-type animals (n=16 wild-type animals; n=24 *daf-18(mg198)* mutant animals). Together, our results indicate that DAF-18 is required for normal morphology in AIY.

DAF-18 acts cell-autonomously in AIY

Pten neuron-specific knockouts in mice result in excessive axon outgrowth and increases in cell size (Backman et al., 2001; Fraser et al., 2004; Kwon et al., 2006; Kwon et al., 2001; van Diepen and Eickholt, 2008). This phenotype is different from that observed in the AIY neurite; a *daf-18* null allele results in shorter AIY neurites. To understand better the role of DAF-18 in AIY, we examined its site of action. To achieve this, we conducted mosaic analysis using a *daf-18* cDNA expressed under the control of its endogenous promoter. Expression of this construct in *daf-18(mg198)* worms resulted in rescue of the AIY neurite length defect. We took advantage of the mitotic instability of the transgene arrays and

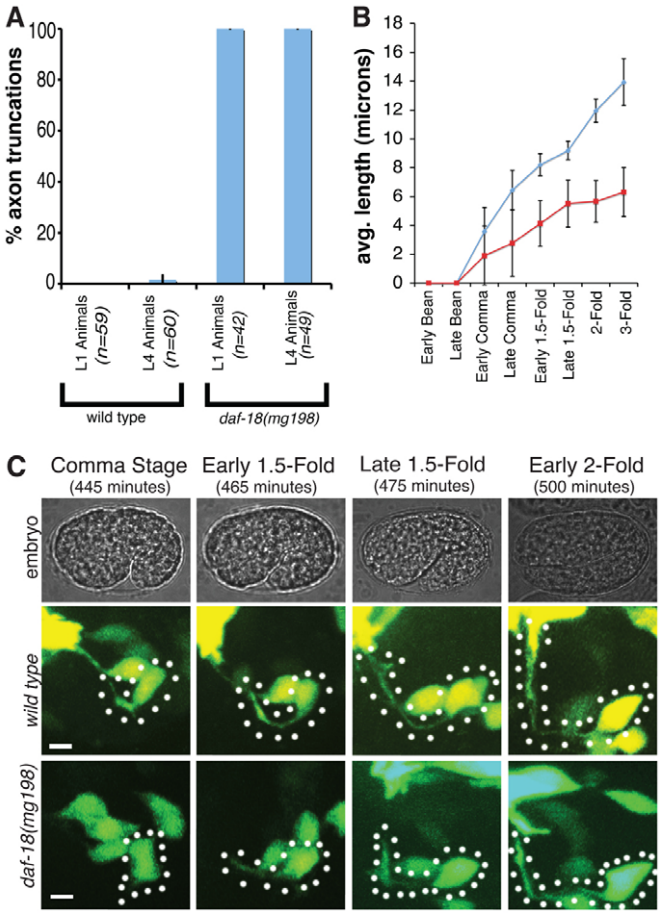

Fig. 2. DAF-18 is required for embryonic neurite outgrowth in AIY. (**A**) Quantification of the percentage of animals with neurite truncations in wild-type and *daf-18(mg198)* larval stage 1 (L1) and larval stage 4 (L4) worms. Note that neurite truncations are already present in *daf-18(mg198)* L1 animals, suggesting that DAF-18 activity is required prior to L1 stage (embryogenesis). (**B**) Average length of the dorsal portion of the AIY neurite in wild-type and *daf-18(mg198)* embryos. Blue, wild type; red, *daf-18(mg198)*. AIY was visualized with cytoplasmic GFP expressed under control of the *ceh-10* and *ttx-3* promoters (Altun-Gultekin et al., 2001; Hobert et al., 1997; Wenick and Hobert, 2004). Average length was calculated from multiple embryos ($n>3$) at the specified developmental stage. (**C**) Transmitted light images and confocal micrographs of comma stage embryos (~445 minutes post-fertilization), early 1.5-fold embryos (~465 minutes post-fertilization), mid 1.5-fold embryos (~475 minutes post-fertilization) and early 2-fold embryos (~500 minutes post-fertilization) for wild-type and *daf-18(mg198)* animals. AIY was visualized using a combinatorial promoter system (*mgIS18 pttx-3b::GFP* and *lqIS4 pceh-10::GFP*). AIY is highlighted with a white dotted line in all images. Note the overall slower rate of neurite elongation in the *daf-18(mg198)* embryos compared with wild-type embryos. Error bars represent s.e.m. Scale bars: 2.5 μm.

analyzed *daf-18(mg198)* mosaic animals retaining the rescuing array in a subset of cells. We observed that mosaic animals retaining the array in AIY were rescued, whereas animals that did not retain the array in AIY, but retained it in other cells, such as postsynaptic partner RIA, were not rescued for the neurite length phenotype in AIY ($P<0.001$) (supplementary material Fig. S2). These mosaic data suggest that DAF-18 acts cell-autonomously in AIY.

To examine further the role of DAF-18 in AIY, we generated transgenic animals that expressed a *daf-18* cDNA from the AIY-specific promoter *ttx-3g* (Wenick and Hobert, 2004). When we examined *daf-18(mg198)* animals expressing this construct, we observed that they were rescued for the neurite length defect in AIY. These results indicate that expression of DAF-18 specifically in AIY is sufficient to rescue the neurite length defects seen in *daf-18(mg198)* mutants (Fig. 1E). Together, our data strongly indicate that DAF-18 acts cell-autonomously in AIY to regulate AIY morphology.

DAF-18 is required for axon outgrowth

We considered three models for how DAF-18/PTEN could function to regulate AIY neurite length: (1) DAF-18 could be required for maintaining AIY neurite length during development, with AIY neurite outgrowth occurring normally during early development, but failing to scale appropriately; (2) DAF-18 activity could be required to prevent neurite degeneration. In this model, AIY neurite outgrowth would occur normally during development, but subsequently atrophy or degenerate; (3) DAF-18 could be required to promote neurite outgrowth during development. To differentiate between these three models we characterized AIY neurite length during development of wild-type and *daf-18* mutant animals.

Larva stage 1 (L1) animals quadruple in size during development to reach adult dimensions (Byerly et al., 1976). During this growth, neurons such as AIY have to appropriately scale to preserve their characteristic morphological features. To determine whether the *daf-18* phenotype resulted from a defect in this scaling process, we examined the AIY phenotype in *daf-18(mg198)* mutant animals during the L1 stage. We observed that *daf-18(mg198)* L1 animals phenocopied *daf-18(mg198)* L4 and adult mutant animals, in both penetrance and expressivity (Fig. 2A). These observations suggest that DAF-18 is not required in AIY for control of scaling during larval growth. Moreover, our data indicate that DAF-18 is required during embryogenesis to mediate AIY neurite length.

Next, we characterized AIY neurodevelopment during embryogenesis. We observed that AIY neurodevelopment is stereotypical across individual animals. The AIY cell body is first visible in bean-stage embryos, ~360 minutes post-fertilization. Neurite outgrowth begins during late bean-stage (~410 minutes post-fertilization), when the nascent growth cone is observed extending from the anterior side of the cell (Fig. 2B,C). Outgrowth continues through the 1.5-fold stage (460 to 490 minutes post-fertilization) until the neurite reaches the dorsal midline (Fig. 2B,C). When the animal has reached the 2-fold stage (490 minutes post-fertilization), AIY neurite extension has concluded and the length of Zone 3 is ~11.5 μm long (Fig. 2B,C). AIY continues to scale in size as the embryo develops, reaching a final length of ~13 μm at the 3-fold stage (550-840 minutes post-fertilization) (Fig. 2B).

In *daf-18(mg198)* mutant animals, many of the early embryonic decisions were made as in wild type. The AIY cell body was first observed and located in the same position as in wild-type embryos. Initiation of neurite outgrowth occurred during the late bean- to comma- stages, and the growth cone extended from the anterior side of the cell (Fig. 2B,C). After outgrowth commenced, we observed that the growth rate of neurites in *daf-18(mg198)* mutants was reduced compared with wild-type animals (Fig. 2C). On average, the growth rate of the AIY neurite in wild-type animals during the bean- to 2-fold stages was 0.17 μm per minute ($n=4$

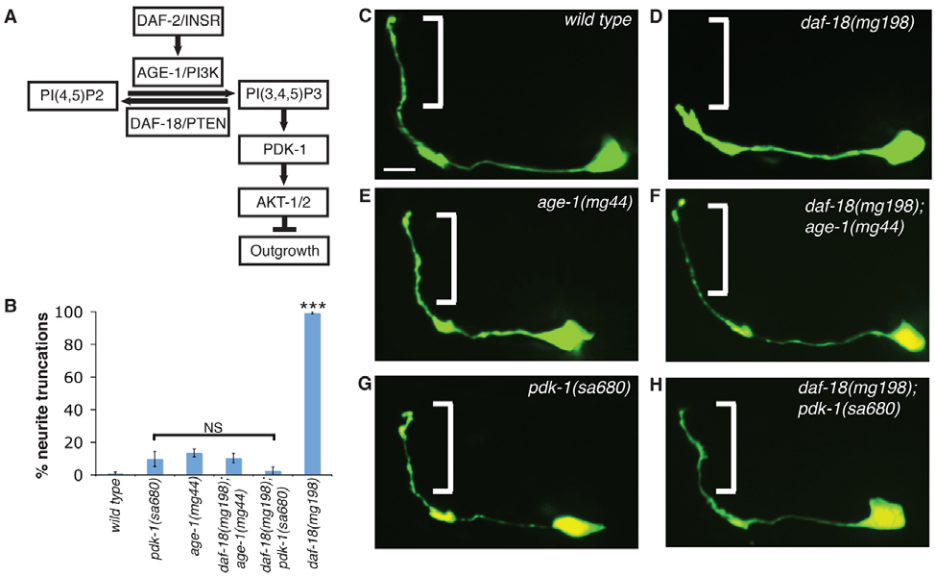

Fig. 3. DAF-18 functions in the PI3K signaling pathway to promote AIY neurite outgrowth. (**A**) Diagram of the PI3K signaling pathway in *C. elegans*. (**B**) Quantification of the percentage of animals with neurite truncations in wild type (*n*=112), *pdk-1(sa680)* mutants (*n*=41), *age-1(mg44)* mutants (*n*=81), *daf-18(mg198); age-1(mg44)* double mutants (*n*=106), *daf-18(mg198); pdk-1(sa680)* double mutants (*n*=46) and *daf-18(mg198)* mutants (*n*=145). Note suppression of neurite truncations in *daf-18(mg198); pdk-1(sa680)* double mutants. (**C-H**) AIY morphology in wild type (C), *daf-18(mg198)* mutant animals (D), *age-1(mg44)* mutant animals (E), *daf-18(mg198); age-1(mg44)* double mutant animals (F), *pdk-1(sa680)* mutant animals (G) and *daf-18(mg198); pdk-1(sa680)* double mutant animals (H) visualized with cytoplasmic GFP expressed cell-specifically in AIY (*pttx-3b::GFP*). Note the missing dorsal portion of neurites in *daf-18(mg198)* animal compared with wild type, and suppression of neurite truncations in the *daf-18(mg198); age-1(mg44)* and *daf-18(mg198); pdk-1(sa680)* double mutants (brackets). ***P<0.001 between indicated groups. NS, not significant. Error bars represent s.e.m. Scale bar: 5 μm.

embryos). The growth rate of the AIY neurite in *daf-18(mg198)* mutant embryos during this time was 0.08 μm per minute (*n*=6 embryos), i.e. half of the growth rate observed for wild-type animals. In adult animals, the difference in neurite length observed between wild type and *daf-18* mutants was about half, consistent with the difference in the embryonic outgrowth rate. Therefore, our data indicate that DAF-18 is required during early embryogenesis for AIY neurite outgrowth.

DAF-18 acts in the PI3K signaling pathway to regulate neuronal morphology

Pten knockout in neurons leads to increases in neurite outgrowth, suggesting that PTEN inhibits outgrowth during development (Backman et al., 2001; Fraser et al., 2004; Kwon et al., 2006; Kwon et al., 2001; van Diepen and Eickholt, 2008). Therefore, our findings demonstrate a novel role for PTEN in promoting neurite outgrowth. To understand better this newfound activity, we set out to identify the signal transduction cascade by which PTEN regulates AIY neurite outgrowth. PTEN is the major negative regulator of the PI3K signaling pathway (Gil et al., 1999; Maehama and Dixon, 1998; McConnachie et al., 2003; van Diepen and Eickholt, 2008). To examine whether PTEN promotes AIY neurite outgrowth by modulating activity of the PI3K pathway, we conducted an epistatic analysis of PTEN and PI3K pathway components.

We examined whether mutations in the PI3K signaling pathway components DAF-2/INSR, AGE-1/PI3K or PDK-1/PDK1 could suppress AIY axon truncations in a *daf-18(mg198)* background. AGE-1 encodes the single *C. elegans* Type 1 PI3K catalytic subunit (Morris et al., 1996) and is believed to be the main source of PIP3 production in *C. elegans*. DAF-2 is the *C. elegans* homolog of insulin/IGF receptors and acts as an upstream activator of AGE-1 activity (Dorman et al., 1995; Kimura et al., 1997). The kinase PDK-1 acts downstream of PIP3 to activate the AKT-1 and AKT-2 kinases and promote PI3K signaling (Fig. 3A) (Alessi et al., 1997; Paradis et al., 1999). We reasoned that if PTEN acts in AIY by inhibiting PI3K signaling, loss-of-function mutations in these genes would suppress the *daf-18* phenotype in AIY. Consistent with DAF-18 acting through the PI3K signaling pathway, we observed that *age-1(mg44)* and *pdk-1(sa680)* suppressed the neurite length defect in *daf-18(mg198)* mutant animals (Fig. 3B-H). In *daf-18* mutants, only 0.7% of animals had wild-type AIY extension (*n*=145) (Fig. 3B). However, we observed that in the *daf-18(mg198); age-1(mg44)* double mutants 89.6% of animals showed wild-type AIY outgrowth (*n*=106) (Fig. 3B,E,F), and 97% of *daf-18(mg198); pdk-1(sa680)* double mutants had wild-type AIY outgrowth (*n*=41) (Fig. 3B,G,H). Surprisingly, a *daf-2(e1370)* mutation failed to suppress AIY neurite truncations (supplementary material Fig. S3C,D). These results are consistent with DAF-18 acting in the PI3K pathway to regulate AIY neurite outgrowth. Our findings also indicate that DAF-2 does not interact genetically with the PI3K signaling pathway in regulation of AIY morphology.

DAF-18 promotes neurite outgrowth through an mTOR-independent pathway

In vertebrates, PTEN can inhibit axon outgrowth through effects on mTOR activity (Kwon et al., 2003; Zhou et al., 2009). In AIY, DAF-18 can promote outgrowth. Although the phenotype in AIY suggests that PI3K signaling inhibits neurite outgrowth in this neuron, we decided to examine whether LET-363/mTOR was also required in regulating AIY outgrowth. We first examined AIY morphology in *let-363(h98)* mutants and observed that AIY

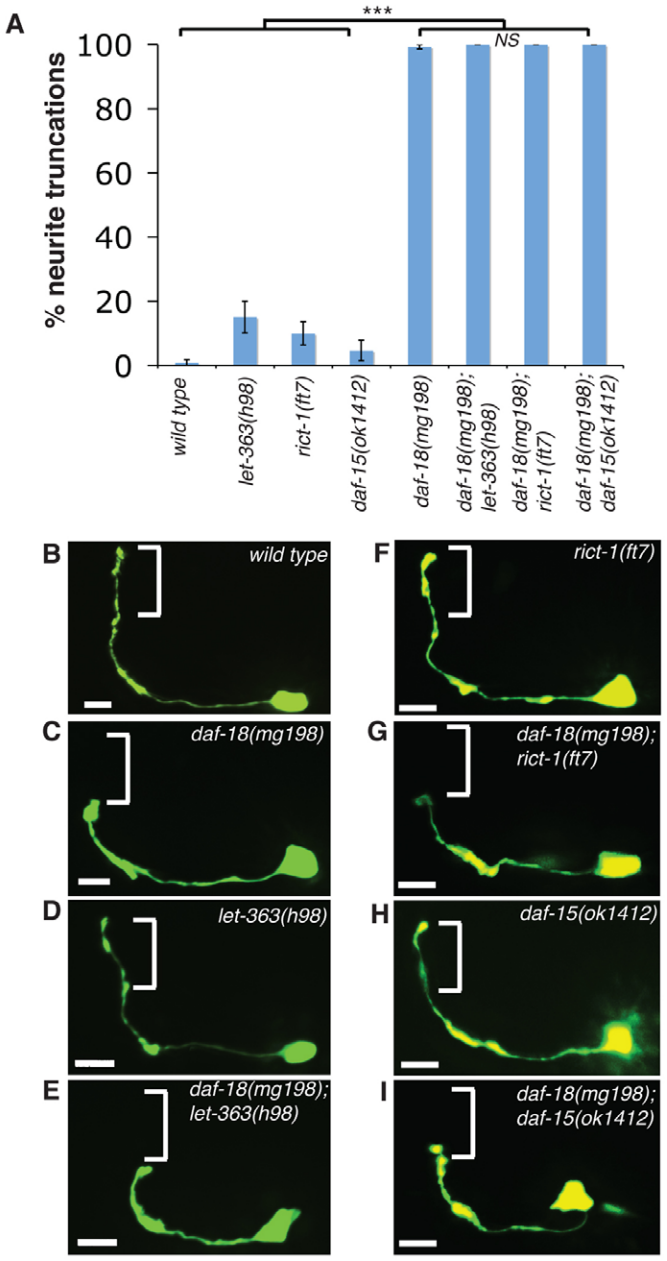

Fig. 4. The LET-363/mTOR pathway is not epistatic to DAF-18 in AIY neurite outgrowth. (**A**) Percentage of animals with neurite truncations in wild type (*n*=112), *let-363(h98) dpy-5(e61) unc-13(e450)* mutants (*n*=53), *rict-1(ft7* mutants*)* (*n*=70), *daf-15(ok1412)* mutants (*n*=43), *daf-18(mg198)* mutants (*n*=145), *daf-18(mg198); let-363(h98) dpy-5(e61) unc-13(e450)* mutants (*n*=55), *daf-18(mg198); rict-1(ft7)* double mutants (*n*=92), *daf-18(mg198); daf-15(ok1412)* double mutants (*n*=60). Note inability of *let-363(h98)*, *rict-1(ft7)* and *daf-15(ok1412)* to suppress AIY neurite truncations in the double mutants. The *let-363(h98) dpy-5(e61) unc-13(e450)* mutant strain was generated by Howell et al. (Howell et al., 1987), and *dpy-5(e61) unc-13(e450)* remain closely linked to *let-363(h98)*. *dpy-5(e61)* and *unc-13(e450)* do not affect AIY development (data not shown). (**B-I**) AIY morphology in wild type (B), *daf-18(mg198)* mutant (C), *let-363(h98) dpy-5(e61) unc-13(e450)* mutant (D), *daf-18(mg198); let-363(h98) dpy-5(e61) unc-13(e450)* mutant (E), *rict-1(ft7)* mutant (F), *daf-18(mg198); rict-1(ft7)* double mutant (G), *daf-15(ok1412)* mutant (H), and *daf-18(mg198); daf-15(ok1412)* double mutant (I), visualized with cytoplasmic GFP expressed cell-specifically in AIY (*pttx-3b::GFP* or *pttx-3g::GFP*). Note the missing dorsal portion of neurites in *daf-18(mg198)* animal compared with *let-363(h98)*, *rict-1(ft7)* and *daf-15(ok1412)* single mutants, and failure of the *let-363(h98)*, *rict-1(ft7)* and *daf-15(ok1412)* mutations to suppress neurite truncations in a *daf-18(mg198)* background (brackets). ***P<0.001. NS, not significant. Error bars represent s.e.m. Scale bars: 5 μm.

development was normal in 85% of animals (*n*=53) (Fig. 4A,D). These data indicate that LET-363 is not a major effector of AIY neurite outgrowth.

We next examined whether LET-363 could inhibit outgrowth downstream of DAF-18. If LET-363 acted to inhibit outgrowth downstream of DAF-18, we reasoned that a loss-of-function mutation in LET-363 would suppress the neurite truncation phenotype in a *daf-18(mg198)* background. To test this hypothesis, we generated a *daf-18(mg198); let-363(h98)* double mutant and examined AIY neurite length. We observed that *daf-18(mg198); let-363(h98)* animals phenocopied *daf-18(mg198)* mutants both in penetrance and expressivity of the AIY neurite truncation defect (*n*=55) (Fig. 4A-E).

Although our results are consistent with LET-363 not affecting AIY outgrowth downstream of the PI3K signaling pathway, we could not rule out the possibility that maternal rescue of LET363 activity during embryogenesis could mask a role in regulating AIY outgrowth (Long et al., 2002). To examine further the role of the mTOR pathway in AIY outgrowth, we probed the role of two mTOR-associated proteins, DAF-15/RPTOR and RICT-1/RICTOR, in AIY development. DAF-15/RPTOR is a conserved regulatory protein of LET-363/mTOR (Kim et al., 2002) that acts downstream of the PI3K signaling pathway (Jia et al., 2004). RICT-1/RICTOR is another LET-363/mTOR-associated regulatory protein acting in the PI3K pathway, where it forms a rapamycin-insensitive complex with mTOR (unlike the rapamycin-sensitive RPTOR/mTOR complex) (Sarbassov et al., 2004; Sarbassov et al., 2005). To examine the requirement of these molecules in AIY neurite outgrowth, we first determined whether they affected AIY development. We observed that 90% of *rict-1(ft7)* mutant animals (*n*=70) and 95% of *daf-15(ok1412)* mutant animals (*n*=43) displayed wild-type AIY neurite extension, demonstrating that neither RICT-1 nor DAF-15 has major effects on AIY neurite outgrowth (Fig. 4A,F,H). We then examined whether RICT-1 or DAF-15 suppressed the DAF-18 phenotype by generating *daf-18(mg198); rict-1(ft7)* and *daf-18(mg198); daf-15(ok1412)* double mutant strains. We observed that 100% of *daf-18(mg198); rict-1(ft7)* (*n*=92) and *daf-18(mg198); daf-15(ok1412)* (*n*=60) animals displayed axon truncations (Fig. 4A,G,I), indicating that these alleles were incapable of suppressing the DAF-18 outgrowth phenotype in AIY. Together, our findings are consistent with LET-363 not acting in the PI3K pathway to inhibit AIY neurite outgrowth.

DAF-16 is required downstream of DAF-18 for outgrowth

DAF-16/FOXO is a conserved transcription factor that regulates multiple physiological processes such as longevity, fat storage, stress response, development and reproduction (Lin et al., 1997; Ogg et al., 1997). DAF-16 is also the major downstream target of

PI3K signaling in *C. elegans* (Lin et al., 1997; Ogg et al., 1997). We therefore examined whether DAF-16 is required for AIY neurite outgrowth downstream of DAF-18.

We first visualized AIY neurodevelopment in *daf-16(mgDF47)* (Ogg et al., 1997) and *daf-16(mu86)* (Lin et al., 1997) null mutants. We observed that *daf-16* mutant animals phenocopied *daf-18* mutants (121 out of 123 *daf-16(mgDF47)* and 77 out of 77 *daf-16(mu86)* animals had AIY neurite truncations) (Fig. 5C; supplementary material Fig. S4C). The *daf-16* phenotype in AIY was qualitatively indistinguishable from that observed for *daf-18* mutant animals (Fig. 5B,C,E). These results indicate that DAF-16 is required for AIY axon outgrowth.

We next examined whether these two molecules act in the same pathway to instruct AIY neurite outgrowth by generating *daf-16(mgDF47); daf-18(mg198)* double mutants. We observed that the neurite outgrowth defect in the *daf-16(mgDF47); daf-18(mg198)* double mutants phenocopied the single mutants; all double mutant animals displayed neurite outgrowth defects (Fig. 5D; data not shown). We also measured the average length of the dorsal portion of the AIY neurite in double mutants and determined that the average neurite length was approximately half of that observed for wild-type animals (wild type: 33.5 µm, 16 animals; *daf-16(mgDF47)*: 17.9 µm, 24 animals; *daf-16(mgDF47); daf-18(mg198)*: 16.1 µm, 32 animals) (Fig. 5E). Our data indicate that *daf-16* and *daf-18* mutants have similar phenotypes in AIY. Our data also indicate that there is no enhancement of the neurite truncation phenotype in *daf-16(mgDF47); daf-18(mg198)* double mutants. Together, our findings suggest that DAF-18/PTEN and DAF-16/FOXO act in the same pathway to promote AIY neurite outgrowth during development.

A specific isoform of DAF-16 is required for developmental neurite outgrowth

Recent studies of DAF-16 demonstrated that specific isoforms of DAF-16 might differentially regulate gene targets to modulate physiological processes in *C. elegans* (Kwon et al., 2010). We therefore hypothesized that the observed role for DAF-16 in promoting AIY neurite outgrowth might be mediated through isoform-specific activity of this transcription factor.

To test this hypothesis, we first examined the isoform-specific loss-of-function allele, *daf-16(mg54)* (Ogg et al., 1997). The *daf-16(mg54)* allele eliminates expression of DAF-16 isoforms A, D and F, but does not affect expression of isoforms B, G or E (supplementary material Fig. S4A). Interestingly, these animals had wild-type AIY outgrowth (supplementary material Fig. S4B). These data indicate that DAF-16 isoforms A, D and F are not required for AIY neurite outgrowth during development.

To characterize further the roles of distinct DAF-16 isoforms in AIY development, we examined AIY morphology in *daf-16* null mutants expressing single isoforms of *daf-16* under the control of isoform-specific upstream sequences (Kwon et al., 2010). Expression of *daf-16b* under the control of its endogenous promoter rescued the AIY neurite truncation defect in *daf-16(mgDF50); daf-2(e1370)* null mutants (n=44 animals) (Fig. 6A,D). By contrast, expression of the *daf-16a* or *daf-16d/f* cDNAs under the control of their endogenous promoters did not result in rescue (n=48 animals for *daf-16a* and n=46 animals for *daf-16d/f*) (Fig. 6B-D). These data are consistent with our observations in *daf-16(mg54)* animals (supplementary material Fig. S4B). Together, our findings indicate that DAF-16A, D and F are not required for AIY neurite outgrowth and that DAF-16B is sufficient to rescue the neurite outgrowth defect in *daf-16* null mutants.

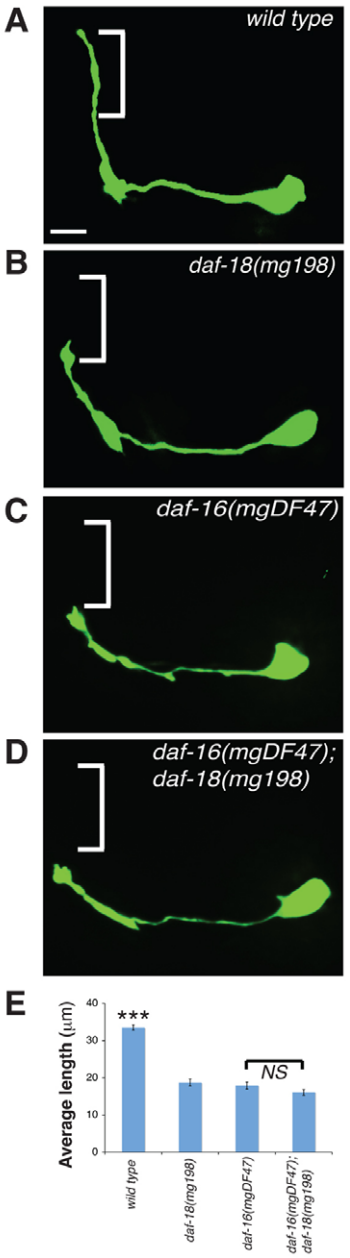

Fig. 5. DAF-16 acts with DAF-18 to promote neurite outgrowth in AIY. (**A-D**) AIY morphology in a wild-type worm (A), *daf-18(mg198)* mutant (B), *daf-16(mgDF47)* mutant (C) and *daf-18(mg198); daf-16(mgDF47)* double mutant (D) visualized with cytoplasmic GFP expressed cell-specifically in AIY (*pttx-3b::GFP*). Note the missing dorsal portion of neurites in *daf-18(mg198), daf-16(mgDF47)* and *daf-16(mgDF47); daf-18(mg198)* double mutant animals compared with the wild-type animal, and the ability of the *daf-16(mgDF47); daf-18(mg198)* double mutant to phenocopy the *daf-16(mgDF47)* and *daf-18(mg198)* single mutants (brackets). (**E**) Average length of the dorsal portion of the AIY neurite in wild type (n=16), *daf-18(mg198)* mutants (n=24), *daf-16(mgDF47)* mutants (n=24) and *daf-16(mgDF47); daf-18(mg198)* double mutants (n=32). ***P<0.001. NS, not significant. Error bars represent s.e.m. Scale bar: 5 µm.

DAF-16B is expressed in neurons (Kwon et al., 2010; Lee et al., 2001; Lin et al., 2001). Based on our findings, we hypothesized that DAF-16B is expressed in AIY to regulate neurite outgrowth downstream of the PI3K signaling pathway. To examine this

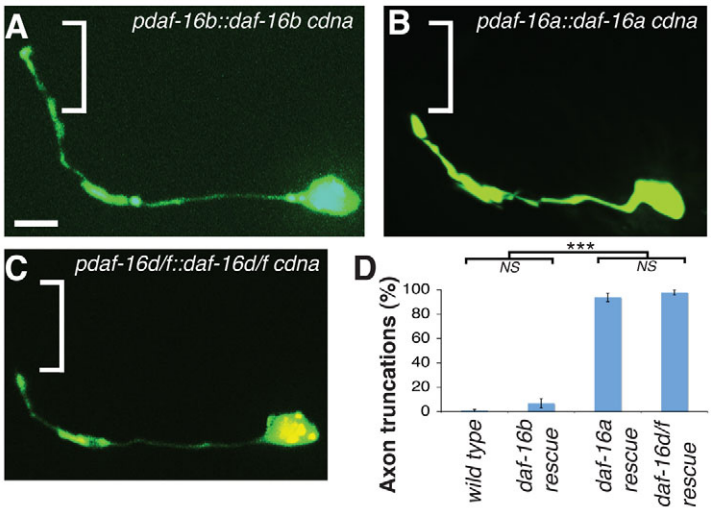

Fig. 6. DAF-16 shows isoform specificity in regulating AIY outgrowth. (**A-C**) AIY morphology in *daf-16(mgDF50); daf-2(e1370)* rescued with *pdaf-16b::daf-16b cDNA* (A), *pdaf-16a::daf-16a cDNA* (B) and *pdaf-16d/f::daf-16d/f cDNA* (C). Note the ability of a *daf-16b cDNA* to rescue neurite truncations in a *daf-16(mgDF50)* background, and the inability of *daf-16a cDNA* and *daf-16d/f cDNA* to do the same. AIY visualized with either GFP (*daf-16a*) or mCH (*daf-16b, daf-16d/f*) expressed cell-specifically in AIY from an extrachromosomal array. The strains used in these rescue experiments were first described by Kwon et al. (Kwon et al., 2010). *daf-2(1370)* does not affect AIY development (supplementary material Fig. S3; data not shown). (**D**) Neurite truncations in wild-type worms (n=112) and *daf-16(mgDF50); daf-2(e1370)* animals rescued with *pdaf-16b::daf-16b cDNA* (n=44), *pdaf-16a::daf-16a cDNA* (n=48) or *pdaf-16d/f::daf-16d/f cDNA* (n=46). Notice the high percentage of neurite truncations in the lines with *pdaf-16a::daf-16a cDNA* and *pdaf-16d/f::daf-16d/f cDNA*, and the complete rescue of neurite truncations in the line with *pdaf-16b::daf-16b cDNA*. Strains shown were first described by Kwon et al. (Kwon et al., 2010), and were injected with a *pttx-3b::GFP* construct during this study. *daf-2(1370)* does not affect AIY development (supplementary material Fig. S3; data not shown). ***P<0.001 between indicated groups. NS, not significant. Error bars represent s.e.m. Scale bar: 5 μm.

hypothesis, we generated transgenic nematodes that expressed GFP under the DAF-16B promoter (*pdaf-16b::gfp*) and mCherry cell-specifically in AIY (*pttx-3g::mCH*). Consistent with our hypothesis, we observed that DAF-16B is expressed in AIY (supplementary material Fig. S5A-C).

We then examined whether DAF-16B acted cell-autonomously to rescue AIY neurite outgrowth. To achieve this, we conducted mosaic analysis using cosmid R13H8 (which contains the complete A and B DAF-16 isoforms, but not D or F isoforms) in *daf-16(mgDF47)* mutant animals. Examination of mosaic animals revealed that animals retaining the array in AIY were rescued for the neurite outgrowth phenotype. Conversely, animals that did not retain the array in AIY, but retained it in other cells, were not rescued for the neurite outgrowth phenotype in AIY (supplementary material Fig. S5D). Together, our data suggest that DAF-16 is expressed in AIY, where it acts downstream of the PI3K signaling pathway to promote neurite outgrowth.

FOXO is required for axon outgrowth in primary cerebellar granule neurons

We next sought to determine whether FOXO proteins have a specific role in axon growth in mammalian neurons, analogously to our findings in *C. elegans*. Within the mammalian brain, granule neurons of the developing cerebellum provide a robust system for the study of axon and dendrite development (Cajal, 1995; Powell et al., 1997). Soon after granule neurons exit mitosis in the external granule layer (EGL), they begin to extend axons that eventually form the parallel fibers of the cerebellar cortex (Altman and Bayer, 1997). Axon growth continues as granule neurons migrate through the molecular and Purkinje cell layers to reach the internal granule layer (IGL). Once in the IGL, granule neurons elaborate dendrites. The stepwise morphogenesis of axons and dendrites is faithfully recapitulated in primary granule neurons, suggesting that granule neurons might harbor cell-intrinsic mechanisms that govern the coordinated growth of axons and dendrites at different stages (de la Torre-Ubieta et al., 2010; Powell et al., 1997).

The FOXO transcription factors have been implicated in the control of polarity in granule neurons (de la Torre-Ubieta et al., 2010). To assess whether FOXO proteins might regulate axon or dendrite growth beyond the stage of polarization, we isolated granule neurons from postnatal day (P) 6 rat pups and transfected the neurons with the U6/foxo RNAi or control U6 RNAi plasmid two days after plating of neurons. Induction of FOXO knockdown in these neurons at a stage after they had already polarized did not substantially increase the number of non-polarized neurons (Fig. 7C). However, FOXO knockdown at this stage dramatically reduced axon length in these neurons compared with control U6-transfected neurons or neurons transfected with one of two different control scrambled shRNAs (Fig. 7A,B). Interestingly, we also observed a concomitant increase in dendrite length (Fig. 7A,B). We confirmed that knockdown of FOXO at this stage had little or no effect on the expression of markers of axons and dendrites (supplementary material Fig. S6A,B). Just as in control neurons, axons in FOXO knockdown neurons expressed the axon marker Tau1, but not the dendrite marker MAP2 (supplementary material Fig. S6A). Conversely, dendrites in FOXO knockdown neurons expressed the dendrite marker MAP2 but not the axon marker Tau1 (supplementary material Fig. S6B). To rule out off-target effects of RNAi, we performed a rescue experiment. Expression of the brain-enriched FOXO protein, FOXO6, encoded by an RNAi-resistant cDNA harboring silent mutations (FOXO6-Res), reversed FOXO RNAi-induced effects on axon and dendrite length in granule

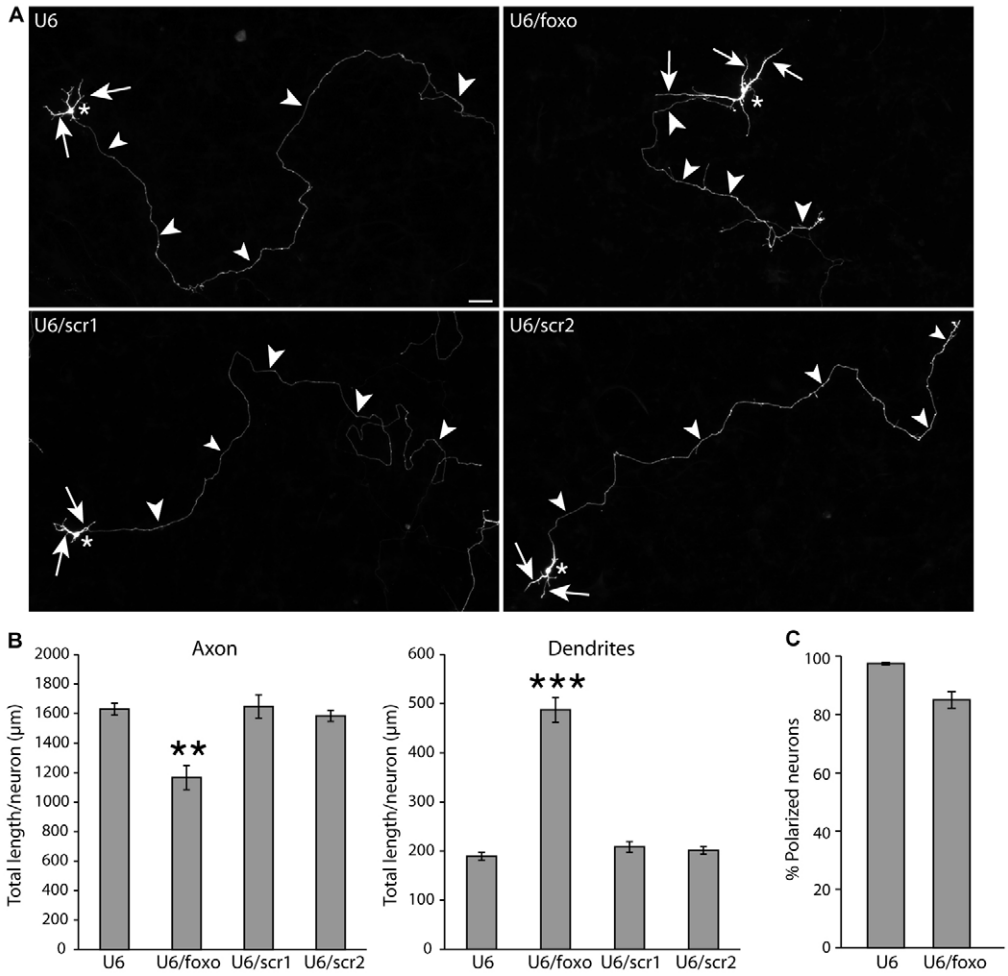

Fig. 7. FOXO proteins regulate the coordinated growth of axons and dendrites. (**A**) Rat cerebellar granule neurons transfected two days after plating with the control U6, the U6/foxo RNAi plasmid, or one of two different scrambled hairpins (U6/scr1 or U6/scr2) and a GFP expression plasmid were subjected four days after transfection to immunocytochemistry with the GFP antibody. Arrows, arrowheads and asterisks indicate dendrites, axons and cell bodies, respectively. Scale bar: 50 μm. (**B**) Morphometric analysis of neurons transfected as in A revealed that FOXO RNAi significantly reduced the length of axons (**P<0.01; ANOVA, 327 neurons measured) and concomitantly increased the length of dendrites (***P<0.001; t-test, 327 neurons measured). (**C**) Granule neurons transfected and analyzed as in A were scored as polarized or non-polarized (as described in Materials and methods). FOXO knockdown in neurons at a stage at which they are already polarized did not substantially affect polarity. Data presented as mean ± s.e.m.

neurons (supplementary material Fig. S7A,B). Together, our data indicate that the FOXO proteins are required for the coordinate morphogenesis of axons and dendrites in granule neurons. Our results also suggest that the FOXO proteins have an evolutionarily conserved role in axon outgrowth and neuronal morphogenesis.

DISCUSSION

Here, we report a novel role for PTEN and FOXO in promoting neurite outgrowth and neuronal morphogenesis during development. We demonstrate that this activity is mediated by a specific isoform of DAF-16, DAF-16B. We also show that the axon growth-promoting function of FOXO is conserved in mammals. Our findings provide a conserved mechanism by which the PI3K signaling pathway regulates outgrowth and controls neuronal morphogenesis.

The PI3K/PTEN signaling pathway is crucial for the correct development of the nervous system (Cosker and Eickholt, 2007; Eickholt et al., 2007; Kwon et al., 2006; Kwon et al., 2003; Kwon et al., 2001; van der Heide et al., 2006; van Diepen and Eickholt, 2008; Waite and Eickholt, 2010; Zhou et al., 2009). In mammals, multiple studies have demonstrated a role for PTEN in inhibiting axon outgrowth by regulating mTOR and protein synthesis (Kwon et al., 2003; Zhou et al., 2009). In the *C. elegans* AIY interneurons, we have observed an additional role for DAF-18/PTEN in promoting neurite outgrowth during development. Our data suggest that this outgrowth promoting activity of PTEN is independent of mTOR activity. We also demonstrate that DAF-18 promotes outgrowth through the transcription factor DAF-16/FOXO. Our findings that the PI3K pathway can inhibit axon outgrowth through the regulation of FOXO transcription factors represents a novel role for PI3K signaling in controlling neurodevelopment.

The FOXO family of transcription factors is conserved throughout evolution (Arden, 2008). FOXOs can control cell proliferation and survival in response to growth factor stimulation (Arden, 2008; Birkenkamp and Coffer, 2003; van der Heide et al., 2006). Although FOXOs are highly expressed in the nervous system of animals (Hoekman et al., 2006), the roles of FOXOs during neurodevelopment remain poorly understood. FOXOs mediate stress-induced neuronal apoptosis (Brunet et al., 1999; Lehtinen et al., 2006; van der Heide et al., 2006; Yuan et al., 2009), and they play prominent roles in neural stem cell proliferation and renewal (Paik et al., 2009). A recent study also demonstrated that these transcription factors, including the nervous system-enriched protein FOXO6, are required for the establishment of neuronal polarity in mammalian neurons (de la Torre-Ubieta et al., 2010). Our findings in *C. elegans* and in mammalian granule cells now demonstrate a conserved role for DAF-16/FOXO in neuronal morphogenesis.

Previous research has demonstrated that different isoforms of DAF-16 have both overlapping and distinct expression patterns and different functional roles (Kwon et al., 2010; Ogg et al., 1997). This research has indicated that DAF-16A is mainly involved in dauer formation and lifespan extension, whereas DAF-16B plays a developmental role in dauer formation (Kwon et al., 2010; Ogg et

al., 1997). The isoforms vary in the DNA-binding domains (Ogg et al., 1997). Together, these findings suggest that the DAF-16 isoforms might have different transcriptional targets to regulate a multiplicity of physiological processes in the worm. Our finding that DAF-16B is sufficient to promote neurite outgrowth in AIY adds neuronal morphogenesis to the known processes regulated by specific DAF-16 isoforms.

The AIY neuron in *C. elegans* is unipolar, and FOXO is required in this neuron for outgrowth. In polarized granule cells, however, we observed that FOXO is both required for axon outgrowth, and to inhibit dendritic length. FOXO had been previously shown to control granule neuron polarity (de la Torre-Ubieta et al., 2010). Nonetheless, we have three lines of evidence which suggest that these newly observed effects of FOXO in axon and dendrite length are likely to be separable from the FOXO-controlled polarity events. First, primary granule neurons undergo a stepwise sequence of neurodevelopmental events (Powell et al., 1997). FOXO knockdown in neurons at a stage after they had already polarized does not substantially alter the number of non-polarized neurons, instead affecting axon and dendrite growth. Second, FOXOs control granule neuronal polarity through polarity protein PAK1 (de la Torre-Ubieta et al., 2010). PAK1 knockdown in neurons at a stage after they had already polarized does not substantially alter the number of non-polarized neurons (data not shown). This result suggests that PAK1 is required for FOXO-mediated polarity but not FOXO-mediated neuronal morphogenesis. Third, *pak-1(ok448)* mutants animals in *C. elegans* do not display any neurite truncation phenotypes that phenocopy those seen for *daf-16* mutants. These data suggest that the differential roles for FOXOs in promoting polarity and axon outgrowth are mediated through distinct downstream effectors. Together, these observations support a model in which FOXO plays three conserved roles in neuron development to regulate neuron morphogenesis: promotion of neuronal polarization, promotion of axon outgrowth and inhibition of dendritic outgrowth.

PTEN/PI3K signaling primarily targets three cellular processes that modulate cellular physiology: (1) cytoskeletal dynamics, (2) protein synthesis and (3) gene transcription (Cosker and Eickholt, 2007; Waite and Eickholt, 2010). PTEN was previously reported to inhibit axon outgrowth through a downstream effector of the PI3K pathway, mTOR (Kwon et al., 2003). Increases in mTOR activity can lead to increases in protein synthesis and concomitant increases in cell size and neurite length. PTEN's capacity to promote axon outgrowth through the FOXO transcription factors now indicates that DAF-18/PTEN can act as an evolutionarily conserved regulator of axon length and neuron morphology, acting to either promote axon outgrowth through promotion of FOXO activity or inhibit it through negative regulation of mTOR.

Acknowledgements
We thank the *Caenorhabditis* Genetic Center and the Japanese NBPR for strains and reagents. We thank Z. Altun (www.wormatlas.org) for diagrams used in the figures. We thank in particular F. Solari for helpful discussions and generous sharing of advice and reagents. We also thank G. Chatterjee for technical assistance and members of the Colón-Ramos laboratory and Alexandra Byrne and Marc Hammarlund from the Hammarlund laboratory for thoughtful comments on the manuscript.

Funding
This work was funded by the National Institutes of Health [R00 NS057931 to D.A.C.-R., NS041021, NS051225 to A.B., 5 T32 GM07499-34 to R.C.]; by the National Science Foundation and the Albert J. Ryan Foundation [L.T.-U.]; and by the Klingenstein Foundation and the Alfred P. Sloan Foundation [D.A.C.-R.]. Deposited in PMC for immediate release.

Competing interests statement
The authors declare no competing financial interests.

Author contributions
R.C. conducted all *C. elegans* experiments and analyzed the resultant data. L.T.-U. conducted all experiments involving primary granule neurons. R.C., L.T.-U., A.B. and D.A.C.-R. wrote the manuscript.

Supplementary material
Supplementary material available online at
http://dev.biologists.org/lookup/suppl/doi:10.1242/dev.069062/-/DC1

References

Adler, C. E., Fetter, R. D. and Bargmann, C. I. (2006). UNC-6/Netrin induces neuronal asymmetry and defines the site of axon formation. *Nat. Neurosci.* **9**, 511-518.
Alessi, D. R., James, S. R., Downes, C. P., Holmes, A. B., Gaffney, P. R., Reese, C. B. and Cohen, P. (1997). Characterization of a 3-phosphoinositide-dependent protein kinase which phosphorylates and activates protein kinase Balpha. *Curr. Biol.* **7**, 261-269.
Altman, J. and Bayer, S. A. (1997). *Development of the cerebellar system: in relation to its evolution, structure, and functions.* Boca Raton: CRC Press.
Altun-Gultekin, Z., Andachi, Y., Tsalik, E. L., Pilgrim, D., Kohara, Y. and Hobert, O. (2001). A regulatory cascade of three homeobox genes, ceh-10, ttx-3 and ceh-23, controls cell fate specification of a defined interneuron class in *C. elegans*. *Development* **128**, 1951-1969.
Arch, E. M., Goodman, B. K., Van Wesep, R. A., Liaw, D., Clarke, K., Parsons, R., McKusick, V. A. and Geraghty, M. T. (1997). Deletion of PTEN in a patient with Bannayan-Riley-Ruvalcaba syndrome suggests allelism with Cowden disease. *Am. J. Med. Genet.* **71**, 489-493.
Arden, K. C. (2008). FOXO animal models reveal a variety of diverse roles for FOXO transcription factors. *Oncogene* **27**, 2345-2350.
Backman, S. A., Stambolic, V., Suzuki, A., Haight, J., Elia, A., Pretorius, J., Tsao, M. S., Shannon, P., Bolon, B., Ivy, G. O. et al. (2001). Deletion of Pten in mouse brain causes seizures, ataxia and defects in soma size resembling Lhermitte-Duclos disease. *Nat. Genet.* **29**, 396-403.
Birkenkamp, K. U. and Coffer, P. J. (2003). Regulation of cell survival and proliferation by the FOXO (Forkhead box, class O) subfamily of Forkhead transcription factors. *Biochem. Soc. Trans.* **31**, 292-297.
Brunet, A., Bonni, A., Zigmond, M. J., Lin, M. Z., Juo, P., Hu, L. S., Anderson, M. J., Arden, K. C., Blenis, J. and Greenberg, M. E. (1999). Akt promotes cell survival by phosphorylating and inhibiting a Forkhead transcription factor. *Cell* **96**, 857-868.
Byerly, L., Cassada, R. C. and Russell, R. L. (1976). The life cycle of the nematode *Caenorhabditis elegans*. I. Wild-type growth and reproduction. *Dev. Biol.* **51**, 23-33.
Cajal, S. R. Y. (1995). *Histology of the nervous system of man and vertebrates.* New York: Oxford University Press.
Colon-Ramos, D. A., Margeta, M. A. and Shen, K. (2007). Glia promote local synaptogenesis through UNC-6 (netrin) signaling in *C. elegans*. *Science* **318**, 103-106.
Cosker, K. E. and Eickholt, B. J. (2007). Phosphoinositide 3-kinase signalling events controlling axonal morphogenesis. *Biochem. Soc. Trans.* **35**, 207-210.
de la Torre-Ubieta, L., Gaudilliere, B., Yang, Y., Ikeuchi, Y., Yamada, T., DiBacco, S., Stegmuller, J., Schuller, U., Salih, D. A., Rowitch, D. et al. (2010). A FOXO-Pak1 transcriptional pathway controls neuronal polarity. *Genes Dev.* **24**, 799-813.
Dorman, J. B., Albinder, B., Shroyer, T. and Kenyon, C. (1995). The age-1 and daf-2 genes function in a common pathway to control the lifespan of *Caenorhabditis elegans*. *Genetics* **141**, 1399-1406.
Eickholt, B. J., Ahmed, A. I., Davies, M., Papakonstanti, E. A., Pearce, W., Starkey, M. L., Bilancio, A., Need, A. C., Smith, A. J., Hall, S. M. et al. (2007). Control of axonal growth and regeneration of sensory neurons by the p110delta PI 3-kinase. *PLoS ONE* **2**, e869.
Fraser, M. M., Zhu, X., Kwon, C. H., Uhlmann, E. J., Gutmann, D. H. and Baker, S. J. (2004). Pten loss causes hypertrophy and increased proliferation of astrocytes in vivo. *Cancer Res.* **64**, 7773-7779.
Gil, E. B., Malone Link, E., Liu, L. X., Johnson, C. D. and Lees, J. A. (1999). Regulation of the insulin-like developmental pathway of *Caenorhabditis elegans* by a homolog of the PTEN tumor suppressor gene. *Proc. Natl. Acad. Sci. USA* **96**, 2925-2930.
Gimm, O., Attie-Bitach, T., Lees, J. A., Vekemans, M. and Eng, C. (2000). Expression of the PTEN tumour suppressor protein during human development. *Hum. Mol. Genet.* **9**, 1633-1639.
Higuchi, M., Onishi, K., Masuyama, N. and Gotoh, Y. (2003). The phosphatidylinositol-3 kinase (PI3K)-Akt pathway suppresses neurite branch formation in NGF-treated PC12 cells. *Genes Cells* **8**, 657-669.
Hobert, O., Mori, I., Yamashita, Y., Honda, H., Ohshima, Y., Liu, Y. and Ruvkun, G. (1997). Regulation of interneuron function in the *C. elegans* thermoregulatory pathway by the ttx-3 LIM homeobox gene. *Neuron* **19**, 345-357.

Hoekman, M. F., Jacobs, F. M., Smidt, M. P. and Burbach, J. P. (2006). Spatial and temporal expression of FoxO transcription factors in the developing and adult murine brain. *Gene Expr. Patterns* **6**, 134-140.
Howell, A. M., Gilmour, S. G., Mancebo, R. A. and Rose, A. M. (1987). Genetic analysis of a large autosomal region in *Caenorhabditis Elegans* by the use of a free duplication. *Genet. Res.* **49**, 207-213.
Jia, K., Chen, D. and Riddle, D. L. (2004). The TOR pathway interacts with the insulin signaling pathway to regulate *C. elegans* larval development, metabolism and life span. *Development* **131**, 3897-3906.
Jia, L., Ji, S., Maillet, J. C. and Zhang, X. (2010). PTEN suppression promotes neurite development exclusively in differentiating PC12 cells via PI3-kinase and MAP kinase signaling. *J. Cell. Biochem.* **111**, 1390-1400.
Kim, D. H., Sarbassov, D. D., Ali, S. M., King, J. E., Latek, R. R., Erdjument-Bromage, H., Tempst, P. and Sabatini, D. M. (2002). mTOR interacts with raptor to form a nutrient-sensitive complex that signals to the cell growth machinery. *Cell* **110**, 163-175.
Kimura, K. D., Tissenbaum, H. A., Liu, Y. and Ruvkun, G. (1997). daf-2, an insulin receptor-like gene that regulates longevity and diapause in *Caenorhabditis elegans*. *Science* **277**, 942-946.
Kodama, E., Kuhara, A., Mohri-Shiomi, A., Kimura, K. D., Okumura, M., Tomioka, M., Iino, Y. and Mori, I. (2006). Insulin-like signaling and the neural circuit for integrative behavior in *C. elegans*. *Genes Dev.* **20**, 2955-2960.
Konishi, Y., Lehtinen, M., Donovan, N. and Bonni, A. (2002). Cdc2 phosphorylation of BAD links the cell cycle to the cell death machinery. *Mol. Cell* **9**, 1005-1016.
Kwon, C. H., Zhu, X., Zhang, J., Knoop, L. L., Tharp, R., Smeyne, R. J., Eberhart, C. G., Burger, P. C. and Baker, S. J. (2001). Pten regulates neuronal soma size: a mouse model of Lhermitte-Duclos disease. *Nat. Genet.* **29**, 404-411.
Kwon, C. H., Zhu, X., Zhang, J. and Baker, S. J. (2003). mTor is required for hypertrophy of Pten-deficient neuronal soma in vivo. *Proc. Natl. Acad. Sci. USA* **100**, 12923-12928.
Kwon, C. H., Luikart, B. W., Powell, C. M., Zhou, J., Matheny, S. A., Zhang, W., Li, Y., Baker, S. J. and Parada, L. F. (2006). Pten regulates neuronal arborization and social interaction in mice. *Neuron* **50**, 377-388.
Kwon, E. S., Narasimhan, S. D., Yen, K. and Tissenbaum, H. A. (2010). A new DAF-16 isoform regulates longevity. *Nature* **466**, 498-502.
Lachyankar, M. B., Sultana, N., Schonhoff, C. M., Mitra, P., Poluha, W., Lambert, S., Quesenberry, P. J., Litofsky, N. S., Recht, L. D., Nabi, R. et al. (2000). A role for nuclear PTEN in neuronal differentiation. *J. Neurosci.* **20**, 1404-1413.
Lee, R. Y., Hench, J. and Ruvkun, G. (2001). Regulation of *C. elegans* DAF-16 and its human ortholog FKHRL1 by the daf-2 insulin-like signaling pathway. *Curr. Biol.* **11**, 1950-1957.
Lehtinen, M. K., Yuan, Z., Boag, P. R., Yang, Y., Villen, J., Becker, E. B., DiBacco, S., de la Iglesia, N., Gygi, S., Blackwell, T. K. et al. (2006). A conserved MST-FOXO signaling pathway mediates oxidative-stress responses and extends life span. *Cell* **125**, 987-1001.
Li, J., Yen, C., Liaw, D., Podsypanina, K., Bose, S., Wang, S. I., Puc, J., Miliaresis, C., Rodgers, L., McCombie, R. et al. (1997). PTEN, a putative protein tyrosine phosphatase gene mutated in human brain, breast, and prostate cancer. *Science* **275**, 1943-1947.
Liaw, D., Marsh, D. J., Li, J., Dahia, P. L., Wang, S. I., Zheng, Z., Bose, S., Call, K. M., Tsou, H. C., Peacocke, M. et al. (1997). Germline mutations of the PTEN gene in Cowden disease, an inherited breast and thyroid cancer syndrome. *Nat. Genet.* **16**, 64-67.
Lin, K., Dorman, J. B., Rodan, A. and Kenyon, C. (1997). daf-16: An HNF-3/forkhead family member that can function to double the life-span of *Caenorhabditis elegans*. *Science* **278**, 1319-1322.
Lin, K., Hsin, H., Libina, N. and Kenyon, C. (2001). Regulation of the *Caenorhabditis elegans* longevity protein DAF-16 by insulin/IGF-1 and germline signaling. *Nat. Genet.* **28**, 139-145.
Long, X., Spycher, C., Han, Z. S., Rose, A. M., Muller, F. and Avruch, J. (2002). TOR deficiency in *C. elegans* causes developmental arrest and intestinal atrophy by inhibition of mRNA translation. *Curr. Biol.* **12**, 1448-1461.
MacDougall, L. K., Domin, J. and Waterfield, M. D. (1995). A family of phosphoinositide 3-kinases in *Drosophila* identifies a new mediator of signal transduction. *Curr. Biol.* **5**, 1404-1415.
Maehama, T. and Dixon, J. E. (1998). The tumor suppressor, PTEN/MMAC1, dephosphorylates the lipid second messenger, phosphatidylinositol 3,4,5-trisphosphate. *J. Biol. Chem.* **273**, 13375-13378.
Marsh, D. J., Dahia, P. L., Zheng, Z., Liaw, D., Parsons, R., Gorlin, R. J. and Eng, C. (1997). Germline mutations in PTEN are present in Bannayan-Zonana syndrome. *Nat. Genet.* **16**, 333-334.
Masse, I., Molin, L., Billaud, M. and Solari, F. (2005). Lifespan and dauer regulation by tissue-specific activities of *Caenorhabditis elegans* DAF-18. *Dev. Biol.* **286**, 91-101.
McConnachie, G., Pass, I., Walker, S. M. and Downes, C. P. (2003). Interfacial kinetic analysis of the tumour suppressor phosphatase, PTEN: evidence for activation by anionic phospholipids. *Biochem. J.* **371**, 947-955.
Mori, I. and Ohshima, Y. (1995). Neural regulation of thermotaxis in *Caenorhabditis elegans*. *Nature* **376**, 344-348.
Morris, J. Z., Tissenbaum, H. A. and Ruvkun, G. (1996). A phosphatidylinositol-3-OH kinase family member regulating longevity and diapause in *Caenorhabditis elegans*. *Nature* **382**, 536-539.
Murakami, H., Bessinger, K., Hellmann, J. and Murakami, S. (2005). Aging-dependent and -independent modulation of associative learning behavior by insulin/insulin-like growth factor-1 signal in *Caenorhabditis elegans*. *J. Neurosci.* **25**, 10894-10904.
Musatov, S., Roberts, J., Brooks, A. I., Pena, J., Betchen, S., Pfaff, D. W. and Kaplitt, M. G. (2004). Inhibition of neuronal phenotype by PTEN in PC12 cells. *Proc. Natl. Acad. Sci. USA* **101**, 3627-3631.
Ogg, S., Paradis, S., Gottlieb, S., Patterson, G. I., Lee, L., Tissenbaum, H. A. and Ruvkun, G. (1997). The Fork head transcription factor DAF-16 transduces insulin-like metabolic and longevity signals in *C. elegans*. *Nature* **389**, 994-999.
Paik, J. H., Ding, Z., Narurkar, R., Ramkissoon, S., Muller, F., Kamoun, W. S., Chae, S. S., Zheng, H., Ying, H., Mahoney, J. et al. (2009). FoxOs cooperatively regulate diverse pathways governing neural stem cell homeostasis. *Cell Stem Cell* **5**, 540-553.
Paradis, S., Ailion, M., Toker, A., Thomas, J. H. and Ruvkun, G. (1999). A PDK1 homolog is necessary and sufficient to transduce AGE-1 PI3 kinase signals that regulate diapause in *Caenorhabditis elegans*. *Genes Dev.* **13**, 1438-1452.
Powell, S. K., Rivas, R. J., Rodriguez-Boulan, E. and Hatten, M. E. (1997). Development of polarity in cerebellar granule neurons. *J. Neurobiol.* **32**, 223-236.
Sarbassov, D. D., Ali, S. M., Kim, D. H., Guertin, D. A., Latek, R. R., Erdjument-Bromage, H., Tempst, P. and Sabatini, D. M. (2004). Rictor, a novel binding partner of mTOR, defines a rapamycin-insensitive and raptor-independent pathway that regulates the cytoskeleton. *Curr. Biol.* **14**, 1296-1302.
Sarbassov, D. D., Guertin, D. A., Ali, S. M. and Sabatini, D. M. (2005). Phosphorylation and regulation of Akt/PKB by the rictor-mTOR complex. *Science* **307**, 1098-1101.
Shi, S. H., Jan, L. Y. and Jan, Y. N. (2003). Hippocampal neuronal polarity specified by spatially localized mPar3/mPar6 and PI 3-kinase activity. *Cell* **112**, 63-75.
Solari, F., Bourbon-Piffaut, A., Masse, I., Payrastre, B., Chan, A. M. and Billaud, M. (2005). The human tumour suppressor PTEN regulates longevity and dauer formation in *Caenorhabditis elegans*. *Oncogene* **24**, 20-27.
van der Heide, L. P., Ramakers, G. M. and Smidt, M. P. (2006). Insulin signaling in the central nervous system: learning to survive. *Prog. Neurobiol.* **79**, 205-221.
van Diepen, M. T. and Eickholt, B. J. (2008). Function of PTEN during the formation and maintenance of neuronal circuits in the brain. *Dev. Neurosci.* **30**, 59-64.
Vanhaesebroeck, B., Leevers, S. J., Panayotou, G. and Waterfield, M. D. (1997). Phosphoinositide 3-kinases: a conserved family of signal transducers. *Trends Biochem. Sci.* **22**, 267-272.
Vanhaesebroeck, B., Leevers, S. J., Ahmadi, K., Timms, J., Katso, R., Driscoll, P. C., Woscholski, R., Parker, P. J. and Waterfield, M. D. (2001). Synthesis and function of 3-phosphorylated inositol lipids. *Annu. Rev. Biochem.* **70**, 535-602.
Waite, K. and Eickholt, B. J. (2010). The neurodevelopmental implications of PI3K signaling. *Curr. Top. Microbiol. Immunol.* **346**, 245-265.
Wenick, A. S. and Hobert, O. (2004). Genomic cis-regulatory architecture and trans-acting regulators of a single interneuron-specific gene battery in *C. elegans*. *Dev. Cell* **6**, 757-770.
White, J. G., Southgate, E., Thomson, J. N. and Brenner, S. (1986). The structure of the nervous system of the nematode *Caenorhabditis elegans*. *Philos. Trans. R. Soc. Lond. B Biol. Sci.* **314**, 1-340.
Yochem, J. and Herman, R. K. (2003). Investigating *C. elegans* development through mosaic analysis. *Development* **130**, 4761-4768.
Yuan, Z., Lehtinen, M. K., Merlo, P., Villen, J., Gygi, S. and Bonni, A. (2009). Regulation of neuronal cell death by MST1-FOXO1 signaling. *J. Biol. Chem.* **284**, 11285-11292.
Zhou, J., Blundell, J., Ogawa, S., Kwon, C. H., Zhang, W., Sinton, C., Powell, C. M. and Parada, L. F. (2009). Pharmacological inhibition of mTORC1 suppresses anatomical, cellular, and behavioral abnormalities in neural-specific Pten knock-out mice. *J. Neurosci.* **29**, 1773-1783.